The Coagulation of Aerosols with Broad Initial Size Distributions

GEORGE W. MULHOLLAND, THOMAS G. LEE, AND HOWARD R. BAUM

National Bureau of Standards, Washington, D.C. 20234

Received June 28, 1976; accepted April 4, 1977

The effect of coagulation on an aerosol with a broad initial size distribution was calculated analytically for large and small particle sizes for arbitrary time with the assumption of a constant coagulation collision frequency. It was found for the class of algebraic initial distributions that there is a long term memory effect so that the large size part of the size distribution is not greatly affected by coagulation. For such distributions the self-preserving hypothesis of Friedlander and Wang does not apply. For a Junge-like initial distribution, which is a special case of an algebraic initial distribution, the size distribution in reduced form is only weakly time dependent and agrees well with measurements on aging smoke generated from smoldering "punk" and flaming α-cellulose. The measured size distributions are found to be in quantitative agreement with the expression, $\psi = 0.1(\eta + 0.1)^{-2}$, where ψ and η are the reduced number distribution and reduced particle volume, respectively.

I. INTRODUCTION

An experimental and theoretical study of the coagulation of smoke aerosols is presented in this paper. While the theoretical work was motivated by the experimental study of smoke aerosols, the results of the calculations are relevant, at least qualitatively, to any aerosol or colloidal system with a broad initial size distribution.

The time evolution of coagulating particles is described by the Smoluchowski equation:

$$\frac{\partial n(v,t)}{\partial t} = \int_0^v \Gamma(v-v',v')n(v-v',t)n(v',t)dv' - 2n(v,t)\int_0^\infty \Gamma(v,v')n(v',t)dv', \quad [1]$$

where $n(v, t)dv$ is the number concentration in the particle volume size range v to $v + dv$, $\Gamma(v, v')$ is the coagulation frequency depending on the sizes v' and v, and t is the time. To fully specify the system an initial condition must be given:

$$n(v, t = 0) = n_0(v). \quad [2]$$

This paper is concerned with the solution of Eq. [1] for the case that $n_0(v)$ is broad, which we define as a type of distribution for which some moment, n_i, of finite order (i finite) fails to exist,

$$n_i \equiv \int_0^\infty v^i n_0(v)dv. \quad [3]$$

We have considered the simplest case for the coagulation frequency, constant Γ. Exact results have been obtained for constant Γ for narrow initial distributions, where narrow means that all the moments of finite order of the distribution exist. The novel feature of our work is the analytic treatment of Eq. [1] for constant Γ for cases where the initial distribution is broad. We show that the nature of the initial size distribution, whether or not it is broad, has a large qualitative effect (as much as orders of magnitude) on the size distribution at later times.

Finding exact solutions to Eq. [1] with constant Γ for various initial conditions has been a problem of some interest through the years. Smoluchowski (1) solved the discrete

Journal of Colloid and Interface Science, Vol. 62, No. 3, December 1977
ISSN 0021-9797

version of Eq. [1] for a monodisperse aerosol, Schumann (2) treated the case

$$n_0(v) \sim e^{-v/v_0}, \qquad [4]$$

and Scott (3) solved Eq. [1] for both a delta function initial condition and for a Gaussian-like distribution,

$$n_0(v) \sim \frac{(\nu+1)^{\nu+1}(v/v_0)^{\nu} \exp\{-(v/v_0)^{\nu+1}\}}{\Gamma(\nu+1)}. \qquad [5]$$

In the above v_0 is a volume constant and ν is an integer.

It has been shown by Wang (4) and by Lushnikov (5) for the case Γ equal to a constant and $n_0(v)$ narrow that the long time asymptotic size distribution is independent of the detailed form of the initial condition,

$$n(v, t) \xrightarrow[t\to\infty]{} \frac{N(t)^2}{V} \exp\{-vN(t)/V\}, \qquad [6]$$

where $N(t)$ is the total number concentration at time t and V is the total volume of the aerosol. Wang claims that the solution is independent of the initial condition without qualifying that the initial distribution be narrow; however, his proof implicitly assumes that all moments of finite order of the initial distribution exists. Lushnikov proved that the asymptotic size distribution is independent of the initial distribution for the discrete version of Eq. [1] provided

$$n_0(v) \leq Ae^{-Bv}, \qquad [7]$$

where A and B are constants.

The major interest in this paper is the effect of a broad initial size distribution on the long time behavior of the size distribution. The class of initial distributions treated here is defined by:

$$n_0(v) = a(v+b)^{-(2+\epsilon)}, \qquad [8]$$

where a, b, and ϵ are constants. For b and ϵ both equal to zero this distribution is known as the Junge size distribution (6).

We find from our analysis that for long time and large particle size the size distribution "remembers" the initial size distribution. The size distribution does not approach the limit given in Eq. [6] for long times as in the case of a narrow initial distribution. The analytic demonstration of this result is a novel contribution of this work; this memory effect for broad distributions is discussed by Junge (Ref. (6, p. 13)) on the basis of a numerical calculation for a specific initial size distribution.

This memory effect also bears directly on the question of the self-preserving hypothesis. The following is based on Wang and Friedlander's (7) statement of this hypothesis. For certain classes of coagulation frequencies

$$\psi(\eta, \tau) \to \psi_1(\eta)$$

after sufficiently long times ($\tau \to \infty$) regardless of the initial form of the size distribution,

$$\psi = \eta(v, t)V/N^2(t), \qquad [9]$$

$$\eta = vN(t)/V, \qquad [10]$$

$$\tau = \Gamma N_0 t.$$

The form of the function $\psi_1(\eta)$ according to the theory of self-preserving size distributions is determined by reducing the partial integro-differential equation (Eq. [1]) to an ordinary integro-differential equation by a similarity transformation. For the case of constant Γ, the similarity solution is identical to the long time asymptotic solution for a narrow initial distribution (Eq. [6]),

$$\psi(\eta) \to e^{-\eta}. \qquad [11]$$

We find that for broad initial size distributions (Eq. [8]) the self-preserving hypothesis is not valid. The size distribution retains its algebraic form for a long time and does not approach the exponential form given in Eq. [11].

Our interest in broad initial size distributions comes from strong evidence for such distributions for combustion-generated aerosols. This evidence includes the studies by Husar (8) on propane flame smoke and our own observations for smoke generated from flaming

α-cellulose (similar to filter paper) and smoldering "punk." We find from our aging studies that the reduced size distributions of "punk" smoke and α-cellulose smoke are very similar, behave as η^{-2} for large η, and are primarily a function of η and virtually independent of the reduced time τ.

The existence of a broad, weakly time dependent size distribution *is* consistent with coagulation theory. For the special case $\epsilon = 0$ in Eq. [8], which corresponds to a Junge-like initial size distribution, ψ is found to be only weakly dependent on τ for τ between 0 and 99 with a shape identical to the experimental shape to the degree of our experimental precision. In other words, we find that coagulation alone is adequate to account for the aging of smoke aerosol provided one uses a realistic initial size distribution.

The effect of the initial size distribution on the long time size distribution has not been widely appreciated. As an aside, we point out that Hidy and Brock's observation (9) concerning the difference between the narrow similarity form and the broad experimentally observed form for atmospheric aerosols can possibly be explained by appreciating that the initial size distribution is broad. As pointed out above, the self-preserving theory simply does not apply to broad initial distributions.

In Section II we present the analysis based on the Laplace transform technique for solving Eq. [1] with the initial condition given by Eq. [8]. The major feature of the calculation is the proper treatment of the branch-point singularity in the Laplace transform of the initial condition. The saddle-point method, which has been used by Scott (3) for calculating the long time, large v solution of Eq. [1], is not applicable to the class of initial distributions given by Eq. [8], because these initial distributions are not analytic. As a guide to the reader interested in the results only, we present the salient features of our analysis in a discussion at the end of Section II.

An electrical aerosol size analyzer was used in measuring the size distribution of the smoke aerosol. Our experimental method and results are presented in Sections III and IV, respectively.

In Section V the validity of the coagulation equation as applied to our experiments is discussed. Specifically, the effect of wall loss, condensation/evaporation, and a size-dependent coagulation coefficient are discussed. Also the implications of the universality of the size distribution of smoke is discussed in light of the calculations.

II. SOLUTION OF COAGULATION EQUATION FOR CONSTANT Γ

For constant Γ, it is convenient to express Eq. [1] in the following form:

$$\frac{\partial\psi(\bar{v}, \lambda)}{\partial\lambda} = \int_0^{\bar{v}} \psi(\bar{v}', \lambda)\psi(\bar{v} - \bar{v}', \lambda)d\bar{v}', \quad [12]$$

where

$$\psi = n(v, t)V/N(t)^2, \quad [13]$$

$$\bar{v} = vN_0/V, \quad [14]$$

$$\lambda = 1 - N(t)/N_0. \quad [15]$$

As has been shown by Scott (3) and Drake (10), the solution of Eq. [12] can be reduced to an integral in the complex plane by using the Laplace transform technique,

$$\psi(\bar{v}, \lambda) = \frac{1}{2\pi i}\int_{\alpha-i\infty}^{\alpha+i\infty} \frac{e^{p\bar{v}}\bar{\psi}_0(p)d\bar{v}}{1 - \lambda\bar{\psi}_0(p)} = \frac{1}{2\pi i}\int_{\alpha-i\infty}^{\alpha+i\infty} e^{p\bar{v}}\bar{\psi}(p)d\bar{v}. \quad [16]$$

The quantity $\bar{\psi}_0(p)$ is the Laplace transform of the initial condition.

In terms of the reduced variables defined by Eqs. [13]–[15], the first two moments of the initial size distribution are unity:

$$\int_0^\infty \psi_0(\bar{v})d\bar{v} = 1, \quad [17]$$

$$\int_0^\infty \bar{v}\psi_0(\bar{v})d\bar{v} = 1. \quad [18]$$

Using these results, we obtain the following expressions for the reduced size distributions corresponding to the initial distributions given by Eq. [8]:

$$\psi(\bar{v}, \lambda = 0) = \epsilon^{1+\epsilon}(1 + \epsilon)(\epsilon + \bar{v})^{-(2+\epsilon)}. \quad [19]$$

For this initial condition, we obtain the following expression for $\bar{\psi}_0(p)$:

$$\bar{\psi}_0(p) = (1 + \epsilon)e^{p\epsilon}\Gamma(-1 - \epsilon)[(p\epsilon)^{1+\epsilon} - \gamma^*(-1 - \epsilon, p\epsilon)], \quad \epsilon \neq \text{integer},$$
$$\bar{\psi}_0(p) = (1 + \epsilon)e^{p\epsilon}E_{2+\epsilon}(p\epsilon), \quad \epsilon = \text{positive integer}. \quad [20]$$

The Γ in Eq. [20] refers to the gamma function and not to the coagulation collision frequency. The function $\gamma^*(a, z)$ is a single valued analytic function of a and z possessing no finite singularities (11). It is related to the incomplete gamma function and its integral representation is

$$\gamma^*(a, z) = \frac{z^{-a}}{\Gamma(a)} \int_0^z e^{-t} t^{a-1} dt. \quad [21]$$

The function $E_m(z)$, the exponential integral, has a logarithmic singularity at $z = 0$,

$$E_m(z) = \int_1^\infty \frac{e^{-zt}}{t^m} dt. \quad [22]$$

The Laplace transforms for the algebraic initial distributions have fundamentally different analytical behavior compared with narrow initial distributions in that they contain branch points at the origin in the complex p plane while the narrow ones have poles. The branch cuts arise due to the appearance of the following expressions in Eq. [20]:

$$(p\epsilon)^{1+\epsilon} \quad \text{for } \epsilon \neq \text{integer},$$
$$\ln(p\epsilon) \quad \text{for } \epsilon = \text{positive integer}.$$

The occurrence of branch cuts is a direct consequence of the nonexistence of all the moments of the initial distribution. This can be readily seen by expanding the Laplace transform of the initial condition $\psi(\bar{v}, \lambda = 0)$ as follows:

$$\bar{\psi}_0(p) = \int_0^\infty \psi(\bar{v}, \lambda = 0)e^{-p\bar{v}} d\bar{v}$$
$$= \int_0^\infty \psi(\bar{v}, \lambda = 0) \sum_{j=0}^\infty \frac{(-p\bar{v})^j}{j!} d\bar{v}$$
$$= \sum_{j=0}^\infty \frac{(-1)^j}{j!} n_j p^j,$$

where

$$n_j \equiv \int_0^\infty \bar{v}^j \psi(\bar{v}, \lambda = 0) d\bar{v}.$$

The last step above can only be carried out if all the moments n_j exist. Conversely, if they do exist and if the growth rate as a function of j is such that the resulting series has a nonzero radius of convergence, the sum defines an analytic function in at least some region about $p = 0$. Hence there can be no branch cuts extending to the origin.

The implications of this difference for the asymptotic solution are quite profound. As will be shown below, the presence of a branch cut gives rise to an algebraic decay to the distribution function considered as a function of $\bar{v}$ in contrast to the exponential decay for the case where $\bar{\psi}_0(p)$ is analytic. Moreover, this algebraic decay is directly related to the initial distribution in contrast to Lushnikov's postulated two stage evolutionary process (12) and to the self-preserving hypothesis, both of which postulate that the initial condition only affects the initial stage of coagulation. The algebraic decay does not, however, violate Lushnikov's theorem, which states that the asymptotic distribution is independent of the initial condition, but rather it lies outside the scope of the theorem (see Eq. [7]).

The inversion theorem can be used to find $\psi(\bar{v}, \lambda)$, since $\bar{\psi}$ vanishes as p approaches infinity in the complex plane. Because of the branch-point singularity in $\bar{\psi}_0(p)$, it is convenient to make use of Cauchy's theorem to express $\psi(\bar{v}, \lambda)$ as a sum of residues plus an integral along the path from A to A' as shown in Fig. 1. With some care it can be shown that

the integrals along the curves ABC and $C'B'A'$ vanish as $|p|$ tends to infinity and the integral around the origin vanishes as $|p|$ tends to zero. We are left with

$$\psi(\bar{v}, \lambda) = \frac{1}{2\pi i}\int_0^\infty e^{-s\bar{v}}\bar{\psi}(se^{-i\pi}, \lambda)ds + \frac{1}{2\pi i}\int_\infty^0 e^{-s\bar{v}}\bar{\psi}(se^{i\pi}, \lambda)ds + 2\pi i \sum \text{Residues}, \quad [23]$$

where $p = se^{\pm i\pi}$ along the negative real axis with the sign determined by which side of the cut (+ upper, − lower) the contour is on. Using Eqs. [16] and [20] and the properties of the functions γ^* and E_n, we can combine the first two integrals in Eq. [23],

$$\psi(\bar{v}, \lambda) = \frac{\Gamma(-\epsilon)\sin[(1+\epsilon)\pi]}{\pi} \times \int_0^\infty \frac{e^{-s\bar{v}}e^{-s\epsilon}(s\epsilon)^{1+\epsilon}ds}{R_1^2 + I_1^2} + 2\pi i \sum \text{Residues}, \quad [24]$$

$$\epsilon \neq \text{integer},$$

$$R_1 = 1 + \lambda e^{-s\epsilon}\Gamma(-\epsilon) \times \{(s\epsilon)^{1+\epsilon}\cos[(1+\epsilon)\pi] - \gamma^*\},$$

$$I_1 = \lambda e^{-s\epsilon}\Gamma(-\epsilon)(s\epsilon)^{(1+\epsilon)} \times \sin[(1+\epsilon)\pi];$$

$$\psi(\bar{v}, \lambda) = \frac{1}{\epsilon!}\int_0^\infty \frac{e^{-s\bar{v}}e^{-s\epsilon}(s\epsilon)^{1+\epsilon}ds}{R_2^2 + I_2^2} + 2\pi i \sum \text{Residues},$$

$$\epsilon = \text{nonzero integer},$$

$$R_2 = 1 - \lambda e^{-s\epsilon}(1+\epsilon) \times \left[A(-s\epsilon) - \ln(s\epsilon)\frac{(s\epsilon)^{1+\epsilon}}{(\epsilon+1)!}\right],$$

$$I_2 = \pi e^{-s\epsilon}(s\epsilon)^{1+\epsilon}/\epsilon!,$$

$$A(z) = E_{2+\epsilon}(z) + \ln z \frac{(-z)^{1+\epsilon}}{(1+\epsilon)!}.$$

So far the result is exact. From this point on, only the asymptotic behavior for large and small $\bar{v}$ will be treated. The analysis is valid for arbitrary λ. Now, the analysis is restricted to the cases $\epsilon = \frac{1}{2}$ and $\epsilon = 0$, both because of the simplicity in analysis and because of the similarity to the experimentally observed size distribution for these cases.

The dominant contribution to $\psi(\bar{v}, \lambda)$ in Eq. [24] for large $\bar{v}$ comes from the first term. It will be shown below that for large $\bar{v}$ the first term in Eq. [24] contributes to $\psi(\bar{v}, \lambda)$ a term proportional to $\bar{v}^{-\frac{5}{2}}$ for $\epsilon = \frac{1}{2}$ and a term proportional to $\bar{v}^{-2}$ for $\epsilon = 0$. The residue terms resulting from poles for $\mathrm{Re}(p) < 0$, if there are any, would be decaying exponentials and for large v would be dominated by the algebraic contribution from the first term. A pole on the imaginary axis could lead to a significant contribution to $\psi(\bar{v}, \lambda)$; however, direct numerical calculations have shown that there are no poles on the imaginary axis and none arbitrarily close to the axis.

$$\epsilon = \tfrac{1}{2}$$

Upon dropping the contribution from poles the behavior for large $\bar{v}$ is obtained from Eq. [24] by making a small s expansion (to order

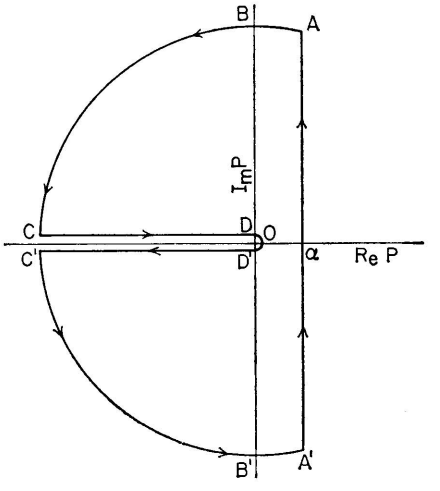

FIG. 1. Contour for integration in the complex plane.

s^2) for the denominator,

$$\psi(\bar{v}, \lambda) = \frac{-\Gamma(-\frac{1}{2})}{\pi} \times \int_0^\infty \frac{e^{-s(\bar{v}+\frac{1}{2})}(s/2)^{\frac{3}{2}}ds}{[(1-\lambda)^2 - 2s\lambda(1-\lambda) + \lambda s^2(2-\lambda)]}. \quad [25]$$

For λ not too close to 1, the integral in Eq. [25] can be approximated by expanding the denominator about $s = 0$:

$$\psi(\bar{v}, \lambda) = \frac{3}{2^{\frac{3}{2}}(\bar{v}+\frac{1}{2})^{\frac{5}{2}}(1-\lambda)} \times \left[1 + \frac{5\lambda}{(\bar{v}+\frac{1}{2})(1-\lambda)}\right]. \quad [26]$$

This approximation is valid provided

$$\lambda \ll (\bar{v}+\tfrac{1}{2})/(\bar{v}+\tfrac{11}{2}).$$

For $\lambda = 0$, Eq. [26] reduces to the initial distribution, Eq. [8] with $\epsilon = \frac{1}{2}$.

In order to obtain a uniform approximation for the integral in Eq. [37] in the limit $\lambda \to 1$, which is equivalent to a long time approximation, we change to the following set of variables:

$$s_1 = s/(1-\lambda),$$
$$\eta = (\bar{v}+\tfrac{1}{2})(1-\lambda).$$

The quantity η defined above approaches the quantity η defined by Eq. [10] in the limit of large $\bar{v}$, which is the case of interest here. In terms of these variables Eq. [25] becomes

$$\psi(\eta, \lambda) = \frac{-\Gamma(-\frac{1}{2})(1-\lambda)^{\frac{1}{2}}}{2^{\frac{3}{2}}\pi} \times \int_0^\infty \frac{e^{-s_1\eta}s_1^{\frac{3}{2}}ds_1}{[1 - 2s_1\lambda + \lambda(2-\lambda)s_1^2]}. \quad [27]$$

Higher-order terms in the denominator of Eq. [27] would be second order in the limit $\lambda \to 1$, because such terms would have a factor $1 - \lambda$.

The important result that $\psi(\eta, \lambda)$ is *not* a self-preserving size distribution is apparent from Eq. [27]. As λ approaches 1, the major time dependence for $\psi(\eta, \lambda)$ comes from the prefactor $(1-\lambda)^{\frac{1}{2}}$, which is approximately $\tau^{-\frac{1}{2}}$ for this range of λ;

$$\tau = \Gamma N_0 t. \quad [28]$$

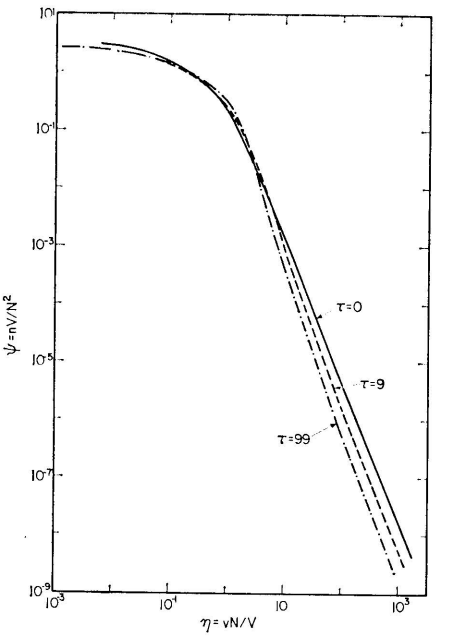

FIG. 2. The calculated reduced size distributions for an initial distribution $\psi_0 = 3[2(\eta + \frac{1}{2})]^{-\frac{3}{2}}$ are plotted for three values of the reduced time τ ($=[N_0/N(t)-1]$).

By a series of changes of variables, the integral in Eq. [27] can be related to the complex error function, W. The final result is

$$\psi(\eta, \lambda) = \frac{(2\pi)^{\frac{1}{2}}(1-\lambda)^{\frac{1}{2}}}{16a_1b_1\lambda(2-\lambda)\eta_1^2} \times \mathrm{Im}\left\{\frac{4z^4W(z) - 2iz/\pi^{\frac{1}{2}} - 4iz^3/\pi^{\frac{1}{2}}}{b_1 - ia_1}\right\}, \quad [29]$$

where

$$W(z) = e^{-z^2}\,\mathrm{erfc}\,(-iz),$$
$$z = \eta^{\frac{1}{2}}(a_1 + ib_1),$$
$$a_1 = \left\{\frac{1}{2(2-\lambda)}\left[1 + \left(\frac{2-\lambda}{\lambda}\right)^{\frac{1}{2}}\right]\right\}^{\frac{1}{2}},$$
$$b_1 = \left\{\frac{1}{2(2-\lambda)}\left[-1 + \left(\frac{2-\lambda}{\lambda}\right)^{\frac{1}{2}}\right]\right\}^{\frac{1}{2}}.$$

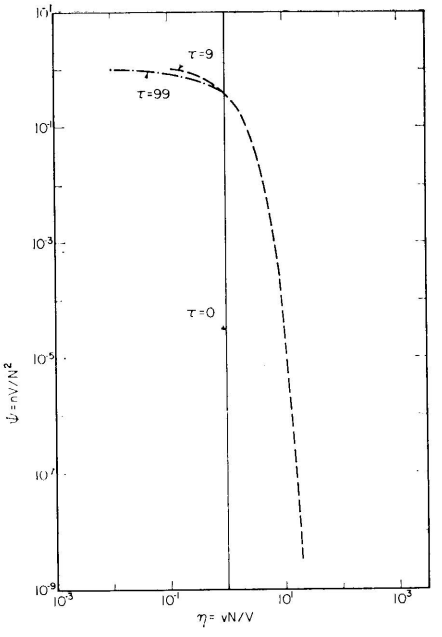

FIG. 3. The calculated reduced size distributions for an initially monodisperse aerosol are plotted for three values of the reduced time. The curves for $\tau = 9$ and $\tau = 99$ are indistinguishable for $\eta > 1$.

Another tactic is used in solving Eq. [1] for small $\bar{v}$. Using the fact that $\bar{\psi}_0(p)$ is analytic for large p (Eq. [20]), we obtain a small $\bar{v}$ expansion for ψ,

$$\psi(\bar{v}, \lambda) = 3[1 - \bar{v}(5 - 3\lambda) + \cdots]. \quad [30]$$

The variable ψ as obtained from Eqs. [29] and [30] is plotted as a function of η for three values of τ in Fig. 2. As stated in the Introduction, ψ does not approach a single, universal size distribution as it does in the case of a narrow initial size distribution. For comparison ψ is plotted in Fig. 3 for an initially monodisperse aerosol. Compared to the monodisperse aerosol the distribution is not nearly so steep for large η. The unreduced size distribution is plotted in Fig. 4. The striking feature of this plot is that for large v the size distribution remains almost invariant with time; it remembers its initial condition. This is in marked contrast to the behavior of a monodisperse aerosol as illustrated in Fig. 5.

$\epsilon = 0$

The case $\epsilon = 0$ is probably the case of greatest interest because of the good agreement with experimental data. This case must be treated differently from the previous case because the aerosol volume, the second moment of the size distribution, is infinite. The unreduced size distribution is, as above, a two parameter distribution,

$$n(v, t = 0) = a_3(v + b_3)^{-2}. \quad [31]$$

One parameter is determined by requiring the first moment of the distribution to equal the total number of aerosol particles. The second parameter is determined below by matching the experimental and calculated size distribution at one point.

In defining reduced variables it is convenient to use the parameter b_3, which has the dimensions of a volume, as a reducing parameter in a way previously used by the ratio V/N_0

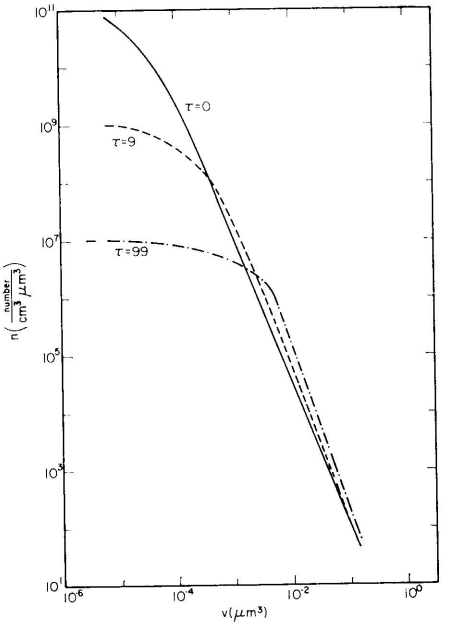

FIG. 4. The number size distributions corresponding to the reduced distributions plotted in Fig. 2 for the case where N_0 and V are equal to the experimental values for smoke from flaming α-cellulose, 2.1×10^6 particles/cm³ and 4.7×10^{-5} μm³, respectively.

(Eqs. [13]-[15]):

$$\psi' = \frac{n(v, t)N_0 b_3}{N(t)^2}, \qquad [32]$$

$$v' = v/b_3. \qquad [33]$$

The initial reduced size distribution is

$$\psi'(v', \lambda = 0) = (v' + 1)^{-2}.$$

Since the analysis is similar to that for the case $\epsilon = \frac{1}{2}$, the emphasis will be on the final results. The expression for $\psi(\bar{v}, \lambda)$, obtained in a manner analogous to that used in obtaining Eq. [25], is

$$\psi(v', \lambda) = \int_0^\infty \frac{e^{-sv'}e^{-s}sds}{[1-\lambda e^{-s}(A(-s)-s\ln s)]^2+\lambda^2 e^{-2s}s^2\pi^2}, \qquad [34]$$

where $A(p) = E_2(p) - p \ln p$.

As in the previous case, we expand the denominator to order s^2 and define reduced variables to isolate the time dependence:

$$s_1 = s/(1 - \lambda),$$
$$\eta' = (v' + 1)(1 - \lambda).$$

The resulting integral may be readily approximated for two limits: large η' and η' of order unity.

The analysis in the case of large η' is similar to that leading to Eq. [26] with the result

$$\psi'(\eta', \lambda) = \frac{1}{\eta'^2}\left\{1 - \frac{4\lambda}{\eta'} \times \left[\ln\left(\frac{1-\lambda}{\eta'}\right) + \tfrac{1}{2}(\tfrac{3}{2} + \gamma)\right]\right\}, \qquad [35]$$

where $\gamma = 0.57721\cdots$ is Euler's constant.

In the case where η' is of order 1, the terms involving $\ln s_1$ in the $\epsilon = 0$ version of Eq. [27] are dropped with the result,

$$\psi'(\eta', \lambda) = \frac{-1}{a\eta' \operatorname{Im}(r_1)} \times \operatorname{Im}\{-\eta' r_1 e^{-\eta' r_1} E(-r_1\eta')\}, \qquad [36]$$

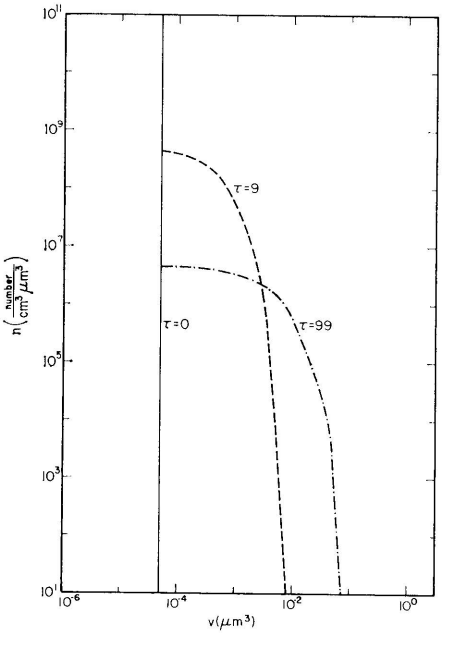

FIG. 5. The number size distributions are plotted for several values of τ for the case of an initial distribution of 2.1×10^6 particles/cm³ all of volume 4.7×10^{-5} μm³.

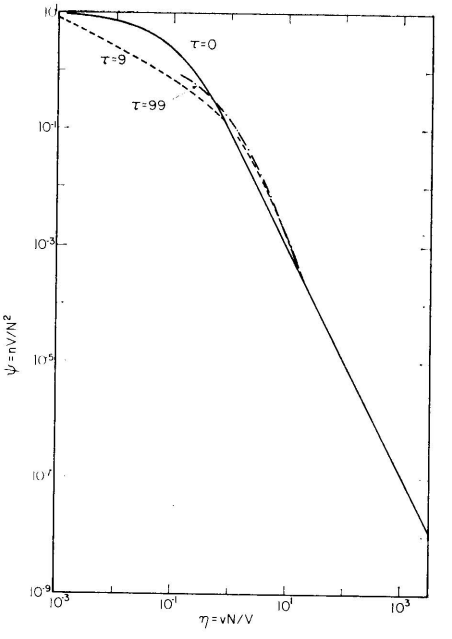

FIG. 6. The calculated reduced size distributions for an initial distribution $\psi_0 = 0.1\ (\eta + 0.1)^{-2}$ are plotted for three values of τ.

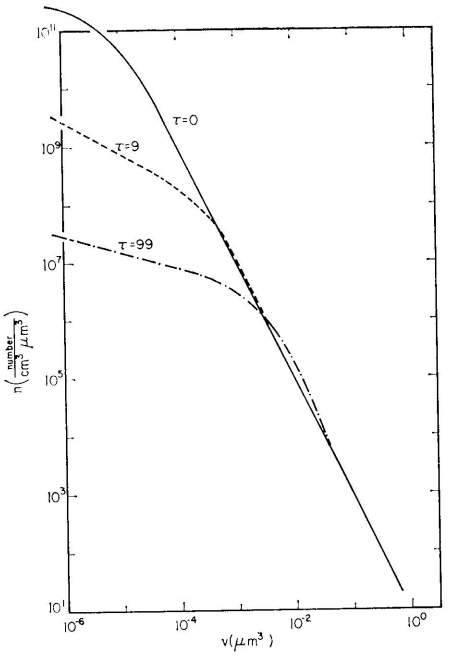

FIG. 7. The number size distributions corresponding to the reduced distributions plotted in Fig. 6 for the case where N_0 and V are equal to the experimental values for smoke from flaming α-cellulose.

where

$$r_1 = \frac{-b + i(4a - b^2)^{\frac{1}{2}}}{2a},$$

$$a = \lambda^2\{\gamma[\ln(1-\lambda) - 1] + \pi^2 + [\ln(1-\lambda)]^2\},$$

$$b = 2\lambda[\gamma + \ln(1-\lambda)].$$

This approximation is best for η' of order 1 and $1 - \lambda \ll 1$.

Finally the result for small v' is found by the same technique as was used in obtaining Eq. [30]:

$$\psi'(v', \lambda) = 1 - v'(2 - \lambda). \qquad [37]$$

The behavior of ψ' for large η' on a log–log plot is similar to the experimental results except that the two curves are displaced from one another. The variables ψ' and η' defined above differ by a factor V/N_0b_3 from ψ and η introduced by Wang and Friedlander (Eqs. [9] and [10]). The ratio $V/(N_0b_3)$ is found to be 10 by requiring the theoretical value of ψ at $\eta = 10$ and $\lambda = 0$ to equal the experimental ψ $(=10^{-3})$ at $\eta = 10$ (see Fig. 9).

As can be seen from Fig. 6 the reduced size distribution curve is a function of only η for large η for the case $\epsilon = 0$. The unreduced size distribution plotted in Fig. 7 is time invariant for large v just as in the case for $\epsilon = \frac{1}{2}$. These two results will be discussed below.

The ψ, η size distributions plotted in Figs. 4 and 6 are accurately calculated for large η (Eqs. [26] and [35]) and for small η (Eqs. [30] and [37]) and are less accurately obtained in the intermediate region (uncertainty about 50%) where Eqs. [29] and [36] plus interpolation are used.

Summary and Discussion of Calculations

We have analytically solved the coagulation equation (Eq. [1]) for the case of a broad initial size distribution and find that the solution is qualitatively different from that of a narrow initial size distribution. This dependence of the long time behavior on the initial condition is physically reasonable. The phenomenon of coagulation is a one-sided process; it allows particles to stick together but does not allow the particles to tear apart. Coagulation can be contrasted with chemical equilibrium where the final state is independent of the initial state. For example, in the chemical reaction,

$$2\,N \rightleftarrows N_2,$$

the same equilibrium state will be reached whether the system is initially all N or all N_2. In coagulation there is no mechanism analogous to N_2 breaking up into two N atoms; thus, the large particles present in the initial distribution will persist for long times.

We have shown that the existence or nonexistence of all finite-order moments of the initial size distribution is the crucial issue concerning the long time behavior of the size distribution. For narrow initial size distributions, the reduced size distribution approaches the limiting value given in Eq. [11]. In Fig. 3

it is shown that ψ has essentially reached the asymptotic form at $\tau = 9$ for an initially monodisperse aerosol.

Our major interest in this study is in the algebraic initial distribution, for which all the moments of finite order do *not* exist. In this case it is the unreduced size distribution $n(v, t)$ that has a simple behavior instead of the reduced distribution $\psi(\eta)$ as above. We find that $n(v, t)$ is almost independent of time for large v (see Fig. 4); in other words, the size distribution remembers its initial condition. This result for the algebraic initial distribution is analytically demonstrated for the case $\epsilon = 0$ and $\epsilon = \frac{1}{2}$ and is likely for any $\epsilon > 0$. The consequence of this steady-state behavior of $n(v, t)$ for large v is that the reduced size distribution is in general a function of both η and the reduced time τ. The case $\epsilon = 0$ is an exception and will be discussed below. Assuming $n(v, t)$ to be steady state for large v for any $\epsilon > 0$, then one finds that with increasing ϵ the time dependence of ψ becomes stronger.

The case $\epsilon = 0$ required special treatment, because the total volume of the aerosol is infinite. It is noteworthy that the size distribution for this case is only a function of η for large η. The reason for the time independent form for large η is a combination of the memory effect of the initial distribution and the algebraic form of the defining equations for the reduced variables ψ and η. The memory effect is likely for any broad initial distribution; however, only for the case $\epsilon = 0$ does the time dependence cancel out of the reduced size distribution. To be more specific if one assumes that the unreduced size distribution is time independent for large particle sizes with a constant slope on a log–log plot, then with simple algebraic manipulations of the reducing factors in Eqs. [9] and [10], one can show that only in the case where the slope is -2 ($\epsilon = 0$) is the size distribution ψ a function of only η for large η. This reasoning is equivalent to that used by Liu and Whitby (13) in arriving at the same result. At that time they thought an additional physical process was necessary for the existence of dynamic equilibrium, $dn/dt = 0$; whereas, we find that dn/dt can be essentially zero for large particle sizes in a system where coagulation is the only dynamic process.

III. EXPERIMENTAL METHOD

This portion of the paper is concerned with the measurement of the size distribution of smoke aerosols at various stages of coagulation. Since the smoke aerosol has a broad initial size distribution smiliar to that assumed in the theoretical calculations in the previous section, we are able to test the validity of the theory for describing the coagulation of real aerosols.

A commercial electrical aerosol analyzer (Thermo-Systems, Inc. Model 3030)[1] was used for measuring the size distribution of smoke aerosols in the size range from less than 0.01 to 1 μm. The performance of the instrument has been described by Liu and Pui (14). While the electrical aerosol analyzer was the primary instrument for this study, we also used a condensation nuclei counter (Environment/One Corporation Model Rich 100)[1] to measure the total number concentration of aerosol particles and a particle mass monitor (Thermo-Systems Model 3200A)[1] to measure the mass concentration of the aerosol.

The two types of smoke studied are the whitish smoke produced by a smoldering "punk" stick and the invisible smoke generated by flaming α-cellulose. "Punk" is a generic term applied to an incense-like material produced in Taiwan for use in religious ceremonies. The stick consists essentially of a bamboo core about 2 mm in diameter covered on the outside by a coating of finely ground natural fiber mixed with chemical oxidant. A typical punk stick was about 3 mm in diameter with a burning rate of about 4 mm/min. It has the con-

[1] Certain commercial materials and equipment are identified in this paper to specify adequately the experimental procedure. In no case does such identification imply recommendation or endorsement by the National Bureau of Standards.

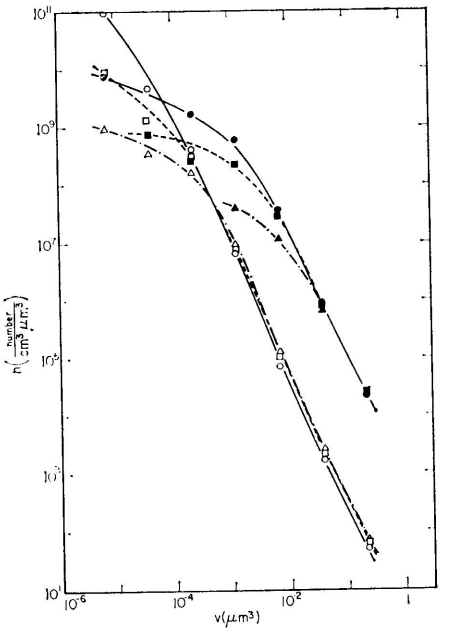

FIG. 8. The measured number distribution of smoke from flaming α-cellulose (○, $\tau = 0$; □, $\tau = 4.5$; △, $\tau = 14$) and of smoke from smoldering "punk" (●, $\tau = 0$; ■, $\tau = 1.4$; ▲, $\tau = 8.1$).

venient property of smoldering in a uniform manner; unfortunately, it does not have a well-defined chemical composition.

The other material is similar to filter paper and consists of pure α-cellulose fibers formed into a 0.8-mm-thick matt. For burning, 5- by 100-mm strips were used.

In the punk smoke experiment 10 punk sticks were set smoldering, placed in the bottom of a 1.8-m^3 cubical box for about 100 sec, and then removed. The large box volume was necessary for minimizing wall losses and dilution resulting from aerosol sampling. The interior surface of the smoke box was made of smooth polymeric sheets. A small fan was positioned inside the box to mix the smoke. By sampling from three different locations in the box, we found that the smoke was well mixed about 2 min after removing the punk sticks from the box.

In the α-cellulose smoke experiment, eight strips of α-cellulose were ignited and then held inside the box for about 40 sec. Care was taken to make sure that all strips were flaming and that they were removed from the box before any one strip had changed from a flaming to a smoldering mode.

After allowing 2 min for the smoke to become well mixed, the size distribution was measured by the electrical aerosol analyzer, the number concentration by a condensation nuclei counter, and the mass concentration by a vibrating quartz crystal mass monitor. The smoke was passed through a charge neutralizer before allowing it to enter the electrical aerosol analyzer. For the first two sets of measurements with the punk smoke, 16 to 1 aerosol diluters (15) were used in the sampling lines going to the electrical aerosol analyzer and the nuclei counter. Typically the size distributions were measured about 2, 30, and 120 min after the smoke source was removed from the box. The total dilution resulting from smoke sampling represented less than 5% of the total volume of the smoke box. No correction was made for this small dilution in the data analysis.

The electrical aerosol analyzer was operated in the least sensitive range (1 V = 10^{-11} A) and was modified to extend the size range to 1 μm by setting the ionizer current at 0.76 $\times$ 10^{-8} A. The switching control was set to skip the first channel, because this channel was slow (25-sec delay) and provided little information in our experiments. To allow additional time for the higher channels to stabilize, we adjusted the 5-sec adjustment potentiometer to allow 7 sec between readings instead of 5. The total scanning time for the 10 channels was 110 sec.

The background aerosol was filtered room air with a typical number concentration of several hundred particles per cubic centimeter (nuclei counter) and with a mass concentration less than 10^{-12} g/cm^3 (mass monitor). It was found empirically that no background corrections were necessary because of the high concentration of the smoke aerosol. The relative humidity was maintained at about 40% and the temperature at 22°C.

IV. RESULTS AND DISCUSSION OF EXPERIMENTAL UNCERTAINTY

In order to compare the experimental results with the model calculations, we have converted the current readings from the electrical aerosol analyzer into values of the size distribution, $dn(v, t)/dv$, by using the calibration factors of Liu and Pui (14). The size distribution of punk smoke and α-cellulose smoke measured at three time intervals are plotted in Fig. 8. Additional data on the two types of smoke are presented in Tables I and II. Both experiments were repeated with almost identical results, except for the punk smoke data in the range $v < 10^{-3}$ μm^3. Because of the small contribution to the total electrical signal from the small size particles in the punk smoke, the signal-to-noise ratio of the output was poor for small particle sizes. Therefore, the punk smoke data for $v < 10^{-4}$ μm^3 are suspect. The α-cellulose data, on the other hand, are repeatable for all the sizes shown.

The most significant observation about the plots is that in both cases the size distributions for the larger sizes are *not* significantly affected by aging. This is in marked contrast to the strong aging effect on the small size portion of the size distribution. Also concerning the large v part of the size distribution, it is noteworthy that the size distribution is a straight line on a log–log plot with a slope slightly less than -2.0. The significance of this slope will be pointed out below.

The fact that the size distribution curve of the punk smoke is on top and to the right of the α-cellulose curve means that the punk smoke particle volume is larger than that of the α-cellulose. After about 2 hr of aging, the average volume ($V/N(t)$) of the punk smoke is 1.8×10^{-2} μm^3 compared to 5.2×10^{-4} μm^3 for the α-cellulose smoke. The corresponding volume mean diameter is 0.32 μm for the smoldering punk smoke compared to 0.10 μm for flaming α-cellulose smoke.

The size distributions are plotted in Fig. 9 in terms of the reduced variables ψ and η. The universal character of the reduced size distribution is striking. Not only the data points at different ages for punk smoke fall on one curve, but also the data points for α-cellulose fall on one curve, which—within experimental

TABLE I

Coagulation of Smoke from Smoldering "Punk"

Time (sec)	τ	N (particles/cm³)	$\bar{v}$ [a] (μm^3)
0	0	2.9×10^6	3.4×10^{-3}
1120	1.4	1.2×10^6	7.1×10^{-3}
7110	8.1	3.2×10^5	1.7×10^{-2}

[a] $\bar{v}$ equals the total volume of aerosol particles divided by the total number of aerosol particles.

TABLE II

Coagulation of Smoke from Flaming α-Cellulose

Time (sec)	τ	N (particles/cm³)	$\bar{v}$ (μm^3)
0	0	2.1×10^6	4.7×10^{-5}
1540	4.5	3.8×10^5	2.1×10^{-4}
6340	14	1.4×10^5	5.2×10^{-4}

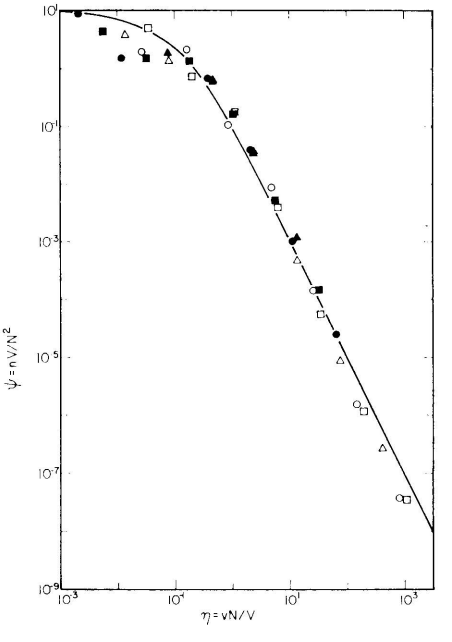

FIG. 9. The reduced size distribution points based on all measured data shown on Fig. 8 and the calculated distribution (solid line) for $\psi = 0.1(\eta + 0.1)^{-2}$.

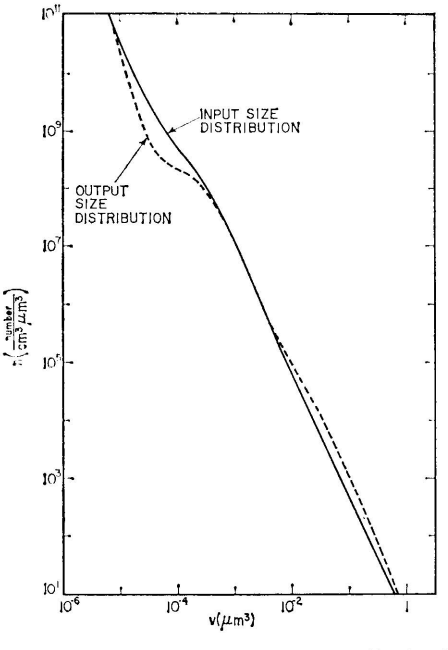

FIG. 10. A comparison of the input size distribution with the output size distribution.

error—is identical with the one for punk smoke!

The accuracy and precision of the electrical aerosol analyzer has not been fully defined; however, a qualitative estimate of the relationship between the true and measured size distribution can be obtained by using the calibration matrix defined by Liu and Pui (14). We assume a certain input size distribution, which corresponds to an array of electrical currents for a perfect instrument, and then operate on this array with the instrument calibration matrix to obtain the output current readings and the corresponding size distribution. A typical input and output size distribution are shown in Fig. 10. The only channel that is significantly distorted by the instrument for this input size distribution is channel 5 ($v = 3.93 \times 10^{-5}$ μm^3). This large distortion can probably be traced to the large jump in electric mobility of a smoke particle as the charge on the particle increases from one charge per particle to two.

The calibration of the electrical aerosol analyzer is based on spherical or near spherical aerosols; if our smoke particles are highly nonspherical, the results may be quite misleading. It is thought that punk smoke is a liquid aerosol so that it would be spherical; less is known about the shape of the α-cellulose smoke generated under flaming conditions.

V. DISCUSSION AND CONCLUSION

Before comparing the experimental results and the model calculations, we consider the validity of applying the coagulation equation to our experiment. Physical processes that might conceivably play an important role in the aging of smoke in addition to coagulation include collisions with the wall, settling, and condensation/evaporation. Empirically we find that the drop in the mass concentration is less than 25% over a 2-hr period during which time the number concentration drops by a factor of at least 10. This small decrease in mass concentration over the 2-hr period indicates that settling is not significant. Even for the largest particle size measured with the electrical aerosol size analyzer, 0.75-μm diameter, the settling process would result in only a 10% drop in mass concentration for that size. If condensation/evaporation were significant mechanisms, then the mass density would increase/decrease with time while the number concentration remained constant.

Additional evidence that condensation/evaporation are not significant mechanisms for punk smoke came from measuring the size distribution for values of the relative humidity over the range 20 to 80%. Changing the humidity had a small effect on the size distribution.

In order to assess the significance of wall loss during the aging experiment a separate experiment was run with a low initial particle concentration, 28,000 particles/cm^3, of punk smoke for a period of 7.2×10^4 sec (20 hr). We obtained a wall loss coefficient, b, of 1.0×10^{-5} sec^{-1} by fitting the experimental number concentration vs time data to an equation obtained by integrating the macroscopic rate equation:

$$dN/dt = -\Gamma N^2 - bN. \qquad [38]$$

This value is within the range of values of b, 7.3×10^{-6} to 1.1×10^{-5} sec^{-1}, reported by Devir (16) for 1.0-μm dioctyl phthalate aerosol in still air. Using the experimentally determined Γ of 4.0×10^{-10} cm^3/sec and b of 1.0×10^{-5}, we find from Eq. [38] that the rate of particle loss from the wall is equal to that from coagulation at a concentration of 2.5×10^4 particles/cm^3. During the coagulation experiment, the number concentration at the end of the experiment was more than five times this number, which means that coagulation was by a factor of five the dominant process even at the end of the experiment. At the start of the experiment this factor was in the range of 80 to 100.

Perhaps the least valid assumption in the model calculation is that the coagulation frequence Γ is size independent. In the continuum regime,

$$\Gamma = \frac{2kT}{3\mu}(D_1 + D_2)\left(\frac{1}{D_1} + \frac{1}{D_2}\right), \quad [39]$$

where D is the particle diameter and μ is the viscosity. Over 80% of the smoke aerosol particles measured have particle sizes within a factor of five or six and, according to Eq. [39], this corresponds to a range of about a factor of two in Γ. It is not expected that the large size part of the size distribution will change qualitatively from the constant Γ case as a result of using a size dependent Γ, because it takes many collisions of small particles with one large one to change its size significantly. On the other hand, one expects a large effect of the form of Γ on the small size part of the distribution. Hidy (17) has shown that for an initially monodisperse aerosol the small size part of the distribution is much more sensitive to the size dependence of Γ than is the large size part.

In any event, a more quantitative statement of the effect of a size dependent Γ on a broad initial size distribution must await a numerical study of the coagulation equation. The major thrust of this study is that a realistic treatment of the initial condition is very important and leads to qualitative agreement with experimental results even for a simplistic choice of the coagulation frequency.

One of the most striking experimental results of this study is the time independence of the size distribution for large v. For an initial condition similar to the experimental one, the coagulation calculation gives the same result. This must be judged as a major success for the calculation.

Another significant experimental result is that the reduced size distribution can be expressed as a function of a single variable. By matching the model calculation to the reduced experimental size distribution at one point, we obtain quantitative agreement between the model calculation and the experimental results. The generality of the theoretical argument that shows that broad self-preserving size distribution must have a slope of -2 adds credibility to the measured size distributions. As shown in Fig. 9, the model size distribution is not strictly time independent for η around 0.1. The experimental accuracy is not adequate to allow one to test the model against the experiment for this range of η. As mentioned above, this is also the size range where one would expect significant deviations from the model calculation because of the assumption of constant Γ.

We find that the reduced experimental size distribution is accurately described by the following formula:

$$\psi = 0.1(\eta + 0.1)^{-2}. \quad [40]$$

This is almost identical to the reduced size distribution of atmospheric aerosols for large η found by Liu and Whitby (13). (The prefactor is 0.07 instead of 0.1.) The corresponding unreduced size distribution is obtained from Eqs. [9] and [10].

$$n(v, t) = 0.1V[v + 0.1V/N(t)]^{-2}. \quad [41]$$

The practical application of Eqs. [40] and [41] to various phases of fire research such as the variation of smoke detector sensitivity with the aging of smoke is of considerable

importance and will be the subject of later studies.

Perhaps the deepest finding of this study is the identification of a basic question: Why does the size distribution of smoke behave as v^{-2} for large particle volume? We have shown that coagulation does not affect the large size part of the size distribution curve. It is up to the theory of smoke formation to answer this question.

ACKNOWLEDGMENTS

The authors wish to recognize Dr. John Rockett for his assistance in discovering a convenient choice of reduced variables for performing the analysis. The authors also wish to thank Ms. Carol Thompson for her conscientious effort in preparing the manuscript.

REFERENCES

1. SMOLUCHOWSKI, M. V., *Z. Phys. Chem.* **92**, 129 (1917).
2. SCHUMANN, T., *Quart. J. Roy. Meteorol. Soc.* **66**, 195 (1940).
3. SCOTT, W. T., *J. Atmos. Sci.* **25**, 54 (1968).
4. WANG, C. S., *J. Inst. Chem. Eng.* **2**, 101 (1971).
5. LUSHNIKOV, A. A., *J. Colloid Interface Sci.* **48**, 400 (1973).
6. JUNGE, C. E., *in* "Advances in Geophysics" (H. E. Landsberg and J. van Mieghem, Eds.), Vol. 4, p. 9. Academic Press, New York, 1958.
7. WANG, C. S., AND FRIEDLANDER, S. K., *J. Colloid Interface Science* **24**, 170 (1967).
8. HUSAR, R., Ph.D. thesis, p. 149. University of Minnesota, 1971.
9. HIDY, G. M., AND BROCK, J. R., "The Dynamics of Aerocolloidal Systems," p. 357. Pergamon, New York, 1970.
10. DRAKE, R. L., *in* "Topics in Current Aerosol Research" (G. M. Hidy and J. R. Brock, Eds.), Vol. 3, Part 2, p. 201. Pergamon, New York, 1972.
11. DAVIS, P. J., *in* "Handbook of Mathematical Functions" (M. Abramowitz and T. Stegun, Eds.), p. 260. Dover, New York, 1968.
12. LUSHNIKOV, A. A., *J. Colloid Interface Sci.* **45**, 549 (1973).
13. LIU, B. Y. H., AND WHITBY, K. T., *J. Colloid Interface Sci.* **26**, 161 (1968).
14. LIU, B. Y. H., AND PUI, D. Y. H., *Aerosol Sci.* **6**, 249 (1975).
15. WHITBY, K. T., LIU, B. Y. H., HUSAR, R. B., AND BARSIC, N. J., *in* "Aerosols and Atmospheric Chemistry" (G. M. Hidy, Ed), p. 199. Academic, New York, 1972.
16. DEVIR, S. E., *J. Colloid Interface Sci.* **18**, 744 (1963).
17. HIDY, G. M., *J. Colloid Sci.* **20**, 123 (1965).